Inorg. Chem. **2008**, *47*, 10081−10089

High Nuclearity Single-Molecule Magnets: a Mixed-Valence Mn_{26} Cluster Containing the Di-2-pyridylketone Diolate Dianion

Theocharis C. Stamatatos,[†,‡] Vassilios Nastopoulos,[†] Anastasios J. Tasiopoulos,[§] Eleni E. Moushi,[§] Wolfgang Wernsdorfer,[⊥] George Christou,*[,‡] and Spyros P. Perlepes*[,†]

Department of Chemistry, University of Patras, Patras 26504, Greece, Department of Chemistry, University of Florida, Gainesville, Florida 32611, Department of Chemistry, University of Cyprus, 1678 Nicosia, Cyprus, and Institut Laboratoire Louis Néel, CNRS & Università J. Fourier, BP-166, Grenoble, Cedex 9, France

Received July 18, 2008

The employment of the dianion ($dpkd^{2-}$) of the *gem*-diol form of di-2-pyridylketone (dpk) as a tetradentate chelate in manganese chemistry is reported, and the synthesis, crystal structure, and magnetochemical characterization of $[Mn_{26}O_{16}(OMe)_{12}(dpkd)_{12}(MeOH)_6](OH)_6 \cdot solv$ (**3** · solv) are described. The reaction of $Mn(ClO_4)_2 \cdot 6H_2O$, dpk, NaOMe, and NEt_3 (2:1:4:2) in MeCN/MeOH affords complex **3**, which possesses a rare metal topology and is mixed-valence ($4Mn^{II}$, $22Mn^{III}$). The complicated $[Mn_{26}(\mu_4\text{-}O)_{10}(\mu_3\text{-}O)_6(\mu_3\text{-}OMe)_{12}(\mu\text{-}OR)_{12}]^{18+}$ core of **3** consists of an internal Mn^{III}_{16} cage of adjacent Mn_4 tetrahedra surrounded by an external $Mn^{II}_4Mn^{III}_6$ shell. The latter is held together by the alkoxide arms of twelve $\eta^1{:}\eta^2{:}\eta^1{:}\eta^1{:}\mu_3$ $dpkd^{2-}$ groups. Variable-temperature, solid-state direct current (dc), and alternating current (ac) magnetization studies were carried out on **3** in the 1.8−300 K range. Complex **3** is predominantly antiferromagnetically coupled with a resulting $S = 6$ ground state, a conclusion confirmed by the in-phase (χ'_M) ac susceptibility data. The observation of out-of-phase (χ''_M) ac susceptibility signals suggested that **3** might be a single-molecule magnet, and this was confirmed by single-crystal magnetization vs dc field sweeps that exhibited hysteresis, the diagnostic property of a magnet. Combined ac χ''_M and magnetization decay vs time data collected below 1.1 K were used to construct an Arrhenius plot; the fit of the thermally activated region above ~0.1 K gave $U_{eff} = 30$ K, where U_{eff} is the effective relaxation barrier. At lower temperatures, the complex exhibits temperature-independent relaxation, characteristic of ground-state quantum tunneling of magnetization between the lowest-lying $M_s = \pm 6$ levels. The combined work demonstrates the ligating flexibility of dipyridyl-diolate chelates and their usefulness in the synthesis of polynuclear Mn_x clusters with interesting magnetic properties, without requiring the co-presence of carboxylate ligands.

Introduction

Interest in polynuclear Mn complexes at moderate oxidation states continues to be high for two main reasons, bioinorganic chemistry and single-molecule magnetism. In the former, the objectives are to model the structures, spectroscopic properties, and/or functions of the active sites of several redox enzymes, the most fascinating of which is the Mn_4Ca cluster that is the water-oxidizing complex (WOC) of green plants and cyanobacteria.[1] In the latter area, polynuclear Mn compounds containing Mn^{III} often have large, and sometimes abnormally large, ground-state spin (S) values, which combined with a large

* To whom correspondence should be addressed. E-mail: christou@chem.ufl.edu (G.C.), perlepes@patreas.upatras.gr (S.P.P.).
† University of Patras.
‡ University of Florida.
§ University of Cyprus.
⊥ Institut Néel, CNRS/UJF.

(1) (a) Ferreira, K. N.; Iverson, T. M.; Maghlaoui, K.; Barber, J.; Iwata, S. *Science* **2004**, *303*, 1831. (b) Carrell, T. G.; Tyryshkin, A. M.; Dismukes, G. C. *J. Biol. Inorg. Chem.* **2002**, *7*, 2. (c) Cinco, R. M.; Rompel, A.; Visser, H.; Aromi, G.; Christou, G.; Sauer, K.; Klein, M. P.; Yachandra, V. K. *Inorg. Chem.* **1999**, *38*, 5988. (d) Yachandra, V. K.; Sauer, K.; Klein, M. P. *Chem. Rev.* **1996**, *96*, 2927. (e) Law, N. A.; Caudle, M. T.; Pecoraro, V. L. In *Advances in Inorganic Chemistry*; Academic Press: Orlando, FL, 1998; Vol. *46*, p 305. (f) Yocum, C. F.; Pecoraro, V. L. *Curr. Opin. Chem. Biol.* **1999**, *3*, 182.
(2) For representative references, see: (a) Christou, G.; Gatteschi, D.; Hendrickson, D. N.; Sessoli, R. *MRS Bull.* **2000**, *25*, 66. (b) Sessoli, R.; Tsai, H.- L.; Schake, A. R.; Wang, S.; Vincent, J. B.; Folting, K.; Gatteschi, D.; Christou, G.; Hendrickson, D. N. *J. Am. Chem. Soc.* **1993**, *115*, 1804.

10.1021/ic801342f CCC: $40.75
Published on Web 10/08/2008

Ising-like magnetoanisotropy (large and negative zero-field splitting parameter, D) have led to some of these species being single-molecule magnets (SMMs).[2] SMMs have a significant energy barrier to magnetization relaxation, and at sufficiently low temperatures will function as nanoscale magnetic particles,[3] with potential applications in information storage and spintronics at the molecular level,[4a] and as quantum bits (qubits) in quantum computation.[4b] They also display quantum effects such as quantum tunneling of the magnetization (QTM)[5] and quantum phase interference.[6] The upper limit to the barrier (U) is given by $S^2|D|$ or $(S^2 - 1/4)|D|$ for integer and half-integer spin, respectively. However, in practice, QTM through upper regions of the anisotropy barrier via higher lying M_s levels of the spin S manifold results in the actual or effective barrier (U_{eff}) being less than U.[2,5] Manganese cluster chemistry has been the main source of new high-spin molecules, but $|D|$ is often too small to give SMMs. Recent examples of complexes with large S but small $|D|$ include $Mn_{28}Cu_{17}$, Mn_{25}, Mn_{19}, and Mn_{10} complexes with $S = 51/2$,[7] 51/2,[8] and 61/2,[9] 83/2,[10] and 44/2[11] ground states, respectively.

We and others have a longstanding interest in alkoxide-based ligands such as the anions of 2-(hydroxymethyl)pyridine ($hmpH$)[9,11a,b,12] and 2,6-pyridinedimethanol ($pdmH_2$)[8,9,13] in Mn cluster chemistry (Scheme 1) as a route to new and interesting clusters. These can form one or two chelate rings per ligand and simultaneously bridge two or more metal atoms. Thus, these and related ligands, for example, the anions of 1,1,1-tris(hydroxymethyl)ethane ($thmeH_3$),[14] triethanolamine ($teaH_3$),[15] *N*-methyldiethanolamine ($mdaH_2$),[16] and others, can foster formation of high nuclearity products. Their alkoxide arm(s) also often support ferromagnetic coupling between the metal ions that they bridge.[8,9,11a,b,12a,b,13a,14–17] These facts have attracted us to further explore alkoxide-containing chelates as a route to new interesting Mn clusters.

Scheme 1. Structures of the Pyridyl-Alcohols Discussed in the Text[a]

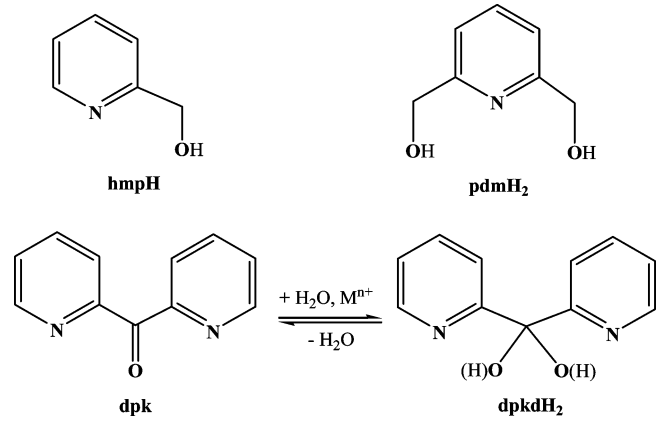

[a] $dpkdH_2$, $dpkdH^-$, and $dkpd^{2-}$ do not exist as free species, only as metal-bound groups.

In the present work, we have explored the use of the potentially tetradentate (N,N',O,O') dianion ($dpkd^{2-}$) of the *gem*-diol form of di-2-pyridylketone (dpk) (Scheme 1); this dianion has previously given a variety of Fe^{II}, Fe^{III}, Co^{II}, Ni^{II}, and Cu^{II} complexes.[18] We considered $dpkd^{2-}$ particularly attractive because it can be considered the fusion of two hmp^- chelates (Scheme 1) that had already proven so useful to us.[9,11a,b,12] Previously reported Mn^{III}-containing products from dpk were $[Mn_{14}O_4(O_2CMe)_{20}(dpkdH)_4]$ ($Mn^{II}_{10}Mn^{III}_4$), containing the monoanion $dpkdH^-$ and pos-

(3) (a) Bircher, R.; Chaboussant, G.; Dobe, D.; Güdel, H. U.; Oshsenbein, S. T.; Sieber, A.; Waldmann, O. *Adv. Funct. Mater.* **2006**, *16*, 209. (b) Gatteschi, D.; Sessoli, R. *Angew. Chem., Int. Ed.* **2003**, *42*, 268. (c) Aubin, S. M. J.; Gilley, N. R.; Pardi, L.; Krzystek, J.; Wemple, M. W.; Brunel, L.- C.; Maple, M. B.; Christou, G.; Hendrickson, D. N. *J. Am. Chem. Soc.* **1998**, *120*, 4991. (d) Oshio, H.; Nakano, M. *Chem.—Eur. J.* **2005**, *11*, 5178.
(4) (a) Bogani, L.; Wernsdorfer, W. *Nat. Mater.* **2008**, *7*, 179. (b) Leuenberger, M. N.; Loss, D. *Nature* **2001**, *410*, 789.
(5) (a) Friedman, J. R.; Sarachik, M. P. *Phys. Rev. Lett.* **1996**, *76*, 3830. (b) Thomas, L.; Lionti, L.; Ballou, R.; Gatteschi, D.; Sessoli, R.; Barbara, B. *Nature* **1996**, *383*, 145.
(6) (a) Wernsdorfer, W.; Sessoli, R. *Science* **2000**, 2417. (b) Wernsdorfer, W.; Soler, M.; Christou, G.; Hendrickson, D. N. *J. Appl. Phys.* **2002**, *91*, 7164. (c) Wernsdorfer, W.; Chakov, N. E.; Christou, G. *Phys. Rev. Lett.* **2005**, *95*, 037203. (1−4).
(7) Wang, W.- G.; Zhou, A.- J.; Zhang, W.- X.; Tong, M.- L.; Chen, X.- M.; Nakano, M.; Beedle, C. C.; Hendrickson, D. N. *J. Am. Chem. Soc.* **2007**, *129*, 1014.
(8) Murugesu, M.; Habrych, M.; Wernsdorfer, W.; Abboud, K. A.; Christou, G. *J. Am. Chem. Soc.* **2004**, *126*, 4766.
(9) Stamatatos, Th. C.; Abboud, K. A.; Wernsdorfer, W.; Christou, G. *Angew. Chem., Int. Ed.* **2007**, *46*, 884.
(10) Ako, A. M.; Hewitt, I. J.; Mereacre, V.; Clérac, R.; Wernsdorfer, W.; Anson, C. E.; Powell, A. K. *Angew. Chem., Int. Ed.* **2006**, *45*, 4926.
(11) (a) Stamatatos, Th. C.; Abboud, K. A.; Wernsdorfer, W.; Christou, G. *Angew. Chem., Int. Ed.* **2006**, *45*, 4134. (b) Stamatatos, Th. C.; Abboud, K. A.; Wernsdorfer, W.; Christou, G. *Polyhedron* **2007**, *26*, 2042. (c) Manoli, M.; Johnstone, R. D. L.; Parsons, S.; Murrie, M.; Affronte, M.; Evangelisti, M.; Brechin, E. K. *Angew. Chem., Int. Ed.* **2007**, *46*, 4456.
(12) (a) Harden, N. C.; Bolcar, M. A.; Wernsdorfer, W.; Abboud, K. A.; Streib, W. E.; Christou, G. *Inorg. Chem.* **2003**, *42*, 7067. (b) Yang, E.- C.; Harden, N.; Wernsdorfer, W.; Zakharov, L.; Brechin, E. K.; Rheingold, A. L.; Christou, G.; Hendrickson, D. N. *Polyhedron* **2003**, *22*, 1857. (c) Boskovic, C.; Brechin, E. K.; Streib, W. E.; Folting, K.; Bollinger, J. C.; Hendrickson, D. N.; Christou, G. *J. Am. Chem. Soc.* **2002**, *124*, 3725. (d) Lecren, L.; Roubeau, O.; Coulon, C.; Li, Y.- G.; Goff, X. F. L.; Wernsdorfer, W.; Miyasaka, H.; Clérac, R. *J. Am.Chem. Soc.* **2005**, *127*, 17353. (e) Lecren, L.; Wernsdorfer, W.; Li, Y.- G.; Roubeau, O.; Miyasaka, H.; Clérac, R. *J. Am. Chem. Soc.* **2005**, *127*, 11311.
(13) (a) Boskovic, C.; Wernsdorfer, W.; Folting, K.; Huffman, J. C.; Hendrickson, D. N.; Christou, G. *Inorg. Chem.* **2002**, *41*, 5107. (b) Brechin, E. K.; Yoo, J.; Huffman, J. C.; Hendrickson, D. N.; Christou, G. *Chem. Commun.* **1999**, 783. (c) Murugesu, M.; Wernsdorfer, W.; Abboud, K. A.; Christou, G. *Polyhedron* **2005**, *24*, 2894. (d) Miyasaka, H.; Nakata, K.; Lecren, L.; Coulon, C.; Nakazawa, Y.; Fujisaki, T.; Sugiura, K.; Yamashita, M.; Clérac, R. *J. Am. Chem. Soc.* **2006**, *128*, 3770. (e) Murugesu, M.; Mishra, A.; Wernsdorfer, W.; Abboud, K. A.; Christou, G. *Polyhedron* **2006**, *25*, 613.
(14) For a representative review, see: (a) Brechin, E. K. *Chem. Commun.* **2005**, 5141, and references therein.
(15) (a) Murugesu, M.; Wernsdorfer, W.; Abboud, K. A.; Christou, G. *Angew. Chem., Int. Ed.* **2005**, *44*, 892, and references therein. (b) Stamatatos, Th. C.; Foguet-Albiol, D.; Wernsdorfer, W.; Abboud, K. A.; Christou, G., to be submitted.
(16) (a) Foguet-Albiol, D.; O'Brien, T. A.; Wernsdorfer, W.; Moulton, B.; Zaworotko, M. J.; Abboud, K. A.; Christou, G. *Angew. Chem., Int. Ed.* **2005**, *44*, 897. (b) Saalfrank, R. W.; Nakajima, T.; Mooren, N.; Scheurer, A.; Maid, H.; Hampel, F.; Trieflinger, C.; Daub, J. *Eur. J. Inorg. Chem.* **2005**, 1149. (c) Foguet-Albiol, D.; Abboud, K. A.; Christou, G. *Chem. Commun.* **2005**, 4282. (d) Wernsdorfer, W.; Stamatatos, Th. C.; Christou, G. *Phys. Rev. Lett.*,submitted for publication.
(17) (a) Yoo, J.; Brechin, E. K.; Yamaguchi, A.; Nakano, M.; Huffman, J. C.; Maniero, A. L.; Brunel, L.- C.; Awaga, K.; Ishimoto, H.; Christou, G.; Hendrickson, D. N. *Inorg. Chem.* **2000**, *39*, 3615. (b) Yang, E.- C.; Hendrickson, D. N.; Wernsdorfer, W.; Nakano, M.; Zakharov, L. N.; Sommer, R. D.; Rheingold, A. L.; Ledezma-Gairraud, M.; Christou, G. *J. Appl. Phys.* **2002**, *91*, 7382.
(18) For a representative review, see: (a) Papaefstathiou, G. S.; Perlepes, S. P. *Comments Inorg. Chem.* **2002**, 249.

sessing a small S value,[19] and the pair $[Mn_{26}O_{16}(OMe)_{12}(dpkd)_{12}(N_3)_6]$ (**1**) and $[Mn_{26}O_{16}(OH)_2(OMe)_{15}(dpkd)_{12}(H_2O)](ClO_4)$ (**2**) that possess similar $Mn^{II}_4Mn^{III}_{22}$ cores, different terminal ligation and ground-state spin values, and behavior suggesting they are SMMs.[20] More recently, we reported that the $Mn/N_3^-/RCO_2^-/dpkd^{2-}$ reaction system gives the covalently linked dimers-of-clusters $[Mn_{24}O_{10}(N_3)_8(O_2CBu^t)_{16}(dpkd)_{12}(DMF)_4]$ and $[Mn_{26}O_8(OH)_4(N_3)_{12}(O_2CMe)_6(dpkd)_{14}(DMF)_4]$, containing $dpkd^{2-}$, both of which are SMMs with relatively large ground-state S values.[21]

We herein report an extension of the use of $dpkd^{2-}$ in nonazide Mn chemistry, which has yielded $[Mn_{26}O_{16}(OMe)_{12}(dpkd)_{12}(MeOH)_6](OH)_6$ (**3**). Complex **3** is another mixed-valence $Mn^{II}_4Mn^{III}_{22}$ complex like **1** and **2** and shows both some similarities and differences with these previously reported complexes. In fact, it allows for interesting comparisons among the three: (i) complex **3** has a different chemical composition from **1** and **2**, illustrating how small changes in the preparative procedures can affect the product identity; (ii) **1**−**3** exhibit slightly different magnetic properties, emphasizing the contribution of the peripheral ligation to the observed magnetic behavior; and (iii) complex **3** has allowed for the first time for this group of $Mn^{II}_4Mn^{III}_{22}$ clusters the observation of hysteresis loops in magnetization versus applied direct current (dc) magnetic field scans, unequivocally establishing the complex to be an SMM.

Experimental Section

Syntheses. All manipulations were performed under aerobic conditions using reagents and solvents as received.

$[Mn_{26}O_{16}(OMe)_{12}(dpkd)_{12}(MeOH)_6](OH)_6$ (3). Method A. To a stirred solution of dpk (0.18 g, 1.0 mmol) and NEt_3 (0.28 mL, 2.0 mmol) in MeCN/MeOH (20/10 mL) was added solid NaOMe (0.22 g, 4.0 mmol). The obtained solution was stirred for 15 min and then solid $Mn(ClO_4)_2\cdot 6H_2O$ (0.72 g, 2.0 mmol) was added under vigorous stirring, which caused a rapid color change from pale yellow to dark brown. The solution was stirred for a further 1 h, filtered, and the filtrate left undisturbed at ambient temperature. After 10 days, X-ray quality dark brown crystals of **3**·solv were collected by filtration, washed with MeCN (2 × 5 mL), and dried in air; the yield was 45%. Anal. Calcd for **3**·3MeCN: C, 38.42; H, 3.53; N, 7.75%. Found: C, 38.84; H, 3.64; N, 7.37%. IR data (KBr, cm^{-1}): 3430 (sb), 1635 (m), 1599 (m), 1566 (w), 1472 (m), 1433 (m), 1384 (w), 1296 (w), 1243 (w), 1212 (w), 1155 (w), 1114 (m), 1076 (s), 1044 (s), 1008 (s), 813 (m), 792 (m), 759 (m), 691 (m), 625 (s), 567 (m), 510 (m).

Method B. To a stirred solution of dpk (0.18 g, 1.0 mmol) and NEt_3 (0.28 mL, 2.0 mmol) in MeCN/MeOH (20/10 mL) was added solid $Mn(ClO_4)_2\cdot 6H_2O$ (0.72 g, 2.0 mmol). The mixture was stirred for 12 h, during which time the color of the solution changed from pale yellow to dark brown. The solution was filtered, and the filtrate left undisturbed at ambient temperature. After 25 days, dark-brown crystals were collected by filtration, washed with MeCN (2 × 5 mL), and dried under vacuum; the yield was 5%. The identity of the product was confirmed by IR spectral comparison with authentic material from Method A.

Table 1. Crystallographic Data for Complex **3**·solv

Formula[a]	$C_{150}H_{162}Mn_{26}N_{24}O_{64}$	T/K	100(2)
M/g mol^{-1}[a]	4753.06	radiation, Å[b]	0.71073
crystal system	cubic	ρ_{calc}, g cm^{-3}	1.513
space group	$Fd\bar{3}$	μ, mm^{-1}	1.589
a, b, c, Å	34.6879(10)	GOF on F^2	1.025
α, β, γ, deg	90	R_1[c,d]	0.0581
V/Å^3	41738(2)	wR_2[e]	0.1404
Z	8	$\Delta\rho_{max,min}$/e Å^{-3}	0.950, −0.509

[a] Solvate molecules have not been included. [b] Mo Kα radiation. [c] $I > 2\sigma(I)$. [d] $R_1 = \sum||F_o| - |F_c||/\sum|F_o|$. [e] $wR_2 = [\sum[w(F_o^2 - F_c^2)^2]/\sum[w(F_o^2)^2]]^{1/2}$, $w = 1/[\sigma^2(F_o^2) + (ap)^2 + bp]$, where $p = [\max(F_o^2, 0) + 2F_c^2]/3$.

X-ray Crystallography. Data were collected on an Oxford Diffraction Xcalibur-3 diffractometer (equipped with a Sapphire CCD area detector) using a graphite-monochromated Mo Kα radiation ($\lambda = 0.71073$ Å). A suitable crystal of **3**·solv was attached to glass fibers using silicone grease and transferred to a goniostat where it was cooled to 100 K for data collection. An initial search for reciprocal space revealed a cubic cell; the choice of space group $Fd\bar{3}$ was confirmed by the subsequent solution and refinement of the structure. Cell parameters were refined using up to 9136 reflections. Data (513 frames) were collected using the ω-scan method (0.75° frame width). Empirical absorption corrections (multiscan based on symmetry-related measurements) were applied using the CRYSALIS RED software.[22] The structure was solved by direct methods using SHELXS-97,[23a] and refined on F^2 using full-matrix least-squares with SHELXL-97.[23b] The non-H atoms were treated anisotropically, whereas the H atoms were placed in calculated, ideal positions and refined as riding on their respective C atoms. The programs used were CRYSALIS CCD[22] for data collection, CRYSALIS RED[22] for cell refinement and data reduction, WINGX[23c] for crystallographic calculations, and MERCURY[23d] for molecular graphics. Unit cell parameters and structure solution and refinement data are listed in Table 1.

For **3**·solv, the asymmetric unit contains $^1/_{12}$ of the Mn_{26} cluster and $^1/_2$ of a OH^- counterion. The six MeOH groups [C(13)−O(7)] coordinated to the Mn(2) atoms are disordered in two positions about the 2-fold axis (50:50 occupancy) as a result of their hydrogen-bonding to one or other of the symmetry-equivalent O2 atoms (O7···O2 = 2.657 Å). There are large voids of ∼6300 Å^3 between the Mn_{26} cations, and these undoubtedly contain solvent of crystallization; however, with the exception of O8, which forms O···H−C contacts with the MeOH groups (O8···C13 = 2.897 Å), other solvent molecules are too disordered to be located. A total of 215 parameters were included in the structure refinement using 3032 reflections with $I > 2\sigma(I)$ to yield R_1 and wR_2 of 5.81 and 14.04%, respectively (CCDC deposition code 691988).

Physical Measurements. Infrared spectra were recorded in the solid state (KBr pellets) on a Nicolet Nexus 670 FTIR spectrometer in the 450−4000 cm^{-1} range. Elemental analyses (C, H, and N) were performed on a Perkin-Elmer 2400 Series II Analyzer. Variable-temperature dc and alternating current (ac) magnetic susceptibility data were collected at the University of Florida using

(19) Milios, C. J.; Kefalloniti, E.; Raptopoulou, C. P.; Terzis, A.; Vicente, R.; Lalioti, N.; Escuer, A.; Perlepes, S. P. *Chem. Commun.* **2003**, 819.
(20) Zaleski, C. M.; Depperman, E. C.; Dendrinou-Samara, C.; Alexiou, M.; Kampf, J. W.; Kessissoglou, D. P.; Kirk, M. L.; Pecoraro, V. L. *J. Am. Chem. Soc.* **2005**, *127*, 12862.
(21) Stamatatos,Th. C.; Abboud, K. A.; Wernsdorfer, W.; Christou, G. *Angew. Chem., Int. Ed.* **2008**, *47*, 6694.
(22) *Oxford Diffraction, CrysAlis CCD and CrysAlis RED*, version 1.171.32.15; Oxford Diffraction Ltd: Abingdon, England, 2008.
(23) (a) Sheldrick, G. M. *SHELXS-97, Program for Crystal Structure Solution*; University of Göttingen: Göttingen, Germany, 1997. (b) Sheldrick, G. M. *SHELXL-97, Program for the Refinement of Crystal Structures from Diffraction Data*; University of Göttingen: Göttingen, Germany, 1997. (c) *WINGX*; Farrugia, L. I. *J. Appl. Crystallogr.* **1999**, *32*, 837. (d) *MERCURY*; Bruno, I. J.; Cole, J. C.; Edgington, P. R.; Kessler, M. K.; Macrae, C. F.; McCabe, P.; Pearson, J.; Taylor, R. *Acta Crystallogr.* **2002**, *B58*, 389.

a Quantum Design MPMS-XL SQUID susceptometer equipped with a 7 T magnet and operating in the 1.8−300 K range. Samples were embedded in solid eicosane to prevent torquing. Alternating current magnetic susceptibility measurements were performed in an oscillating ac field of 3.5 G and a zero dc field. The oscillation frequencies were in the 50−997 Hz range. Pascal's constants were used to estimate the diamagnetic corrections, which were subtracted from the experimental susceptibilities to give the molar paramagnetic susceptibilities (χ_M). Low-temperature (<1.8 K) hysteresis studies and dc relaxation measurements were performed at Grenoble using an array of micro-SQUIDS.[24] The high sensitivity of this magnetometer allows the study of single crystals of SMMs of the order of 10−500 μm. The field can be applied in any direction by separately driving three orthogonal coils. Crystals were maintained in mother liquor to avoid degradation and were covered with grease for protection during transfer to the micro-SQUID and subsequent cooling.

Results and Discussion

Syntheses. In the presence of carboxylate groups, pyridyl alcohols such as hmpH, the related 2-(hydroxyethyl)pyridine (hepH), and $pdmH_2$ have given products such as certain Mn_{10},[12a] Mn_{18},[25] and Mn_4[17a] complexes, respectively. In the absence of carboxylates, Mn_{10},[11a,b] Mn_{25},[8] and Mn_7[26] products, respectively, have resulted. For the present work, we have concentrated on non-carboxylate reactions, and a number have been investigated differing in the Mn starting material, the Mn:dpk:NEt_3 ratio, and/or the solvent. The reaction of $Mn(ClO_4)_2 \cdot 6H_2O$, dpk, NEt_3, and NaOMe in a 2:1:2:4 ratio in MeCN/MeOH (Method A) gave a dark brown solution and subsequent isolation of $[Mn_{26}O_{16}(OMe)_{12}(dpkd)_{12}(MeOH)_6](OH)_6$ (**3**) in ~45% yields; its formation is summarized in eq 1.

$$26Mn^{2+} + 12dpk + 18MeO^- + 28NEt_3 + \frac{11}{2}O_2 + 17H_2O \rightarrow [Mn_{26}O_{16}(OMe)_{12}(dpkd)_{12}(MeOH)_6]^{6+} + 28NHEt_3^+ \quad (1)$$

The reaction is an oxidation, undoubtedly by O_2 under the prevailing basic conditions, and has been balanced accordingly. Note that the reactions of dpk with 3d metal ions have been well studied over the years,[18] and it is known that water and ROH can add to the carbonyl group of metal-bound dpk to give $dpkdH_2$ (the *gem*-diol form of dpk; Scheme 1) and dpkd(R)H (the hemiacetal form of dpk), respectively. If the NaOMe is omitted and an increased amount of NEt_3 is used to facilitate generation of MeO^- in situ (Method B), only a very low (5%) yield of complex **3** is obtained. In the absence of both NEt_3 and NaOMe, only pale yellow solutions indicative of Mn^{II} species were obtained; we have not pursued characterization of these products. Similarly, an increase in the amount of dpk to 2 equiv (or more) again gave yellow solutions that retained their color even after 48 h stirring in air. The MeCN/MeOH solvent ratio of Method A could be varied over a wide range and still gave **3**, although the 2:1 ratio gave the highest yield and most crystalline product. Neat MeCN, however, gave only very low yields (<5%) of impure **3**.

(24) Wernsdorfer, W. *Adv. Chem. Phys.* **2001**, *118*, 99.

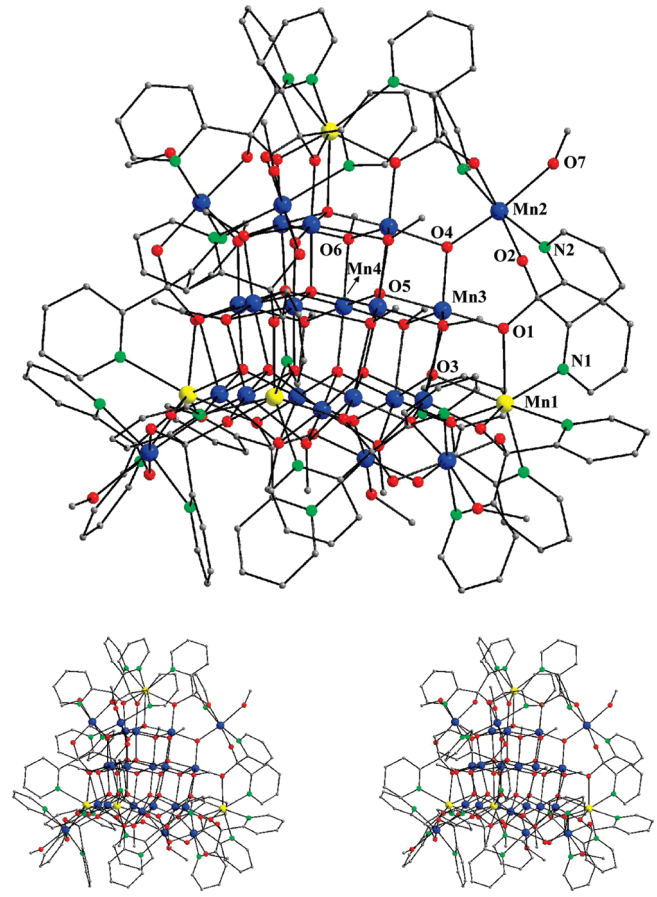

Figure 1. Labeled PovRay representation (top) and stereopair (bottom) of complex **3**, with H atoms omitted for clarity. Color scheme: Mn^{II}, yellow; Mn^{III}, blue; O, red; N, green; C, gray.

Description of Structure. A partially labeled plot and a stereoview of the cation of complex **3** are shown in Figure 1. Selected interatomic distances and angles are listed in Table 2. Complex **3** crystallizes in the cubic space group $Fd\bar{3}$. The complicated structure of the $[Mn_{26}O_{16}(OMe)_{12}(dpkd)_{12}(MeOH)_6]^{6+}$ cation consists of an internal Mn_{16} cage within an external Mn_{10} shell. The former (Figure 2, top) consists of sixteen Mn^{III} atoms (Mn3, Mn4, and their symmetry equivalents) arranged as three layers of three, six, and seven Mn atoms connected by μ_4-O^{2-} atoms O5, μ_3-OMe^- atoms O6, four μ_3-O^{2-} atoms O3 (which become μ_4 by also linking to Mn1 in the outer Mn_{10} shell), and μ-O^{2-} atoms O4 (which become μ_3 by also linking to Mn2 in the outer Mn_{10} shell). The μ_4-O^{2-} atoms O5 are very distorted from tetrahedral geometry (Mn−μ_4-O^{2-}−Mn angles range from 96.7(1) to 139.8(3)°), and the μ_3-O^{2-} (O4) atoms are distorted trigonal planar (largest Mn−O−Mn angle of 128.0(1)°). The twelve $[Mn_3(\mu_3\text{-}OMe^-)]^{8+}$ and six $[Mn_3(\mu_3\text{-}O^{2-})]^{7+}$ units are close to (Mn3···Mn4 = 3.122(1) Å, Mn3′···Mn4 = 3.110(1) Å, Mn3···Mn3′= 3.237(1) Å) or exactly (Mn2···Mn3 = 3.390(1) Å, Mn2···Mn3′ = 3.390(1) Å, Mn3···Mn3′ = 2.945(1) Å) isosceles, the long separations corresponding to ones not bridged by a μ_4-O^{2-} ion.

The external Mn_{10} unit (Figure 2, bottom) consists of four Mn^{II} (Mn1) and six Mn^{III} (Mn2) atoms and encapsulates the internal Mn_{16} cage. The connections between the alternating Mn^{II}/Mn^{III} atoms are by the alkoxide arms of $dpkd^{2-}$ groups.

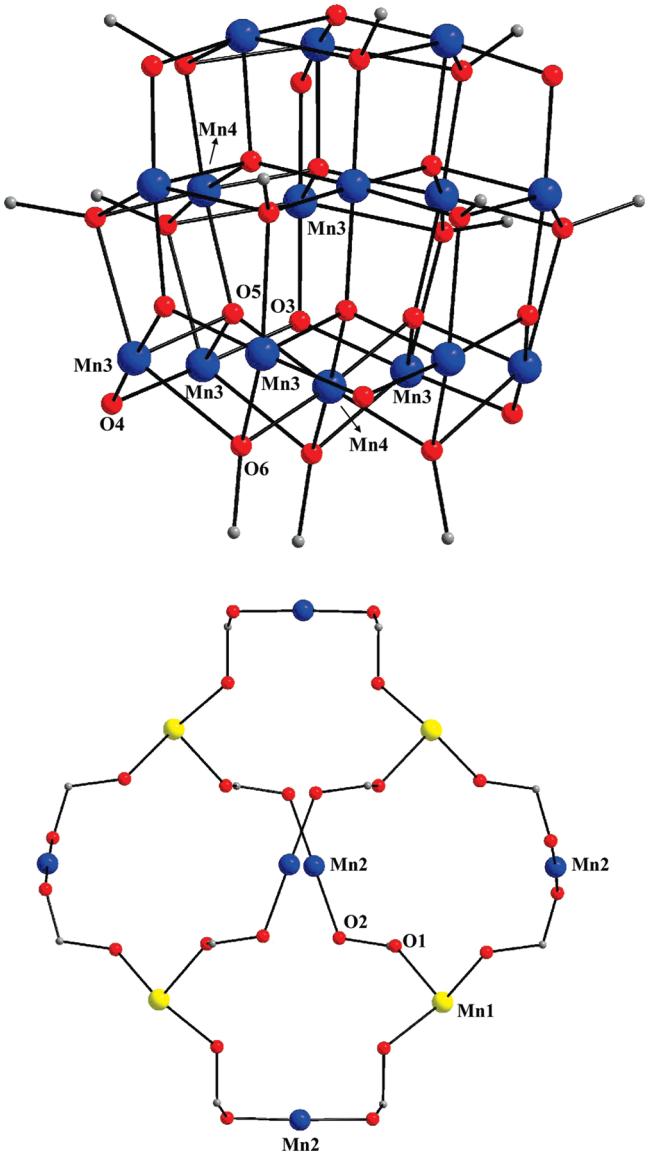

Figure 2. Labeled PovRay representation of the internal Mn_{16} core (top) and the external Mn_{10} shell (bottom) of complex **3**. Color scheme: Mn^{II}, yellow; Mn^{III}, blue; O, red; C, gray.

Table 2. Selected Interatomic Distances (Å) and Angles (deg) for Complex **3**

Mn(1)−Mn(2)	5.658(1)	Mn(2)−Mn(3)	3.390(1)
Mn(1)−Mn(3)	3.334(1)	Mn(2)−Mn(4)	5.392(1)
Mn(1)−Mn(4)	5.561(1)	Mn(3)−Mn(4)	3.122(1)
Mn(1)−O(1)	2.217(4)	Mn(3)−O(3)	1.909(2)
Mn(1)−O(3)	2.366(6)	Mn(3)−O(4)	1.870(3)
Mn(1)−N(1)	2.404(6)	Mn(3)−O(5)	1.969(3)
Mn(2)−O(2)	1.910(4)	Mn(3)−O(6)	2.296(4)
Mn(2)−O(4)	1.900(5)	Mn(3)−O(6)	2.306(4)
Mn(2)−O(7)	2.115(1)	Mn(4)−O(5)	2.005(2)
Mn(2)−N(2)	2.270(5)	Mn(4)−O(6)	2.006(4)
Mn(3)−O(1)	1.905(4)		
Mn(1)−O(1)−Mn(3)	107.7(2)	Mn(3)−O(6)−Mn(3)	89.4(2)
Mn(1)−O(3)−Mn(3)	101.9(2)	Mn(3)−O(5)−Mn(4)	103.5(7)
Mn(2)−O(4)−Mn(3)	128.0(1)	Mn(3)−O(5)−Mn(4)	102.9(7)
Mn(3)−O(3)−Mn(3)	115.9(1)	Mn(3)−O(6)−Mn(4)	92.5(2)
Mn(3)−O(4)−Mn(3)	103.9(2)	Mn(4)−O(5)−Mn(4)	139.6(3)
Mn(3)−O(5)−Mn(3)	96.9(2)		

The latter are doubly-*N*,*O* bidentate-chelating to two adjacent Mn atoms (Mn1 and Mn2), with one of their alkoxide arms (O1) also bridging to a central Mn^{III} atom (Mn3); these groups

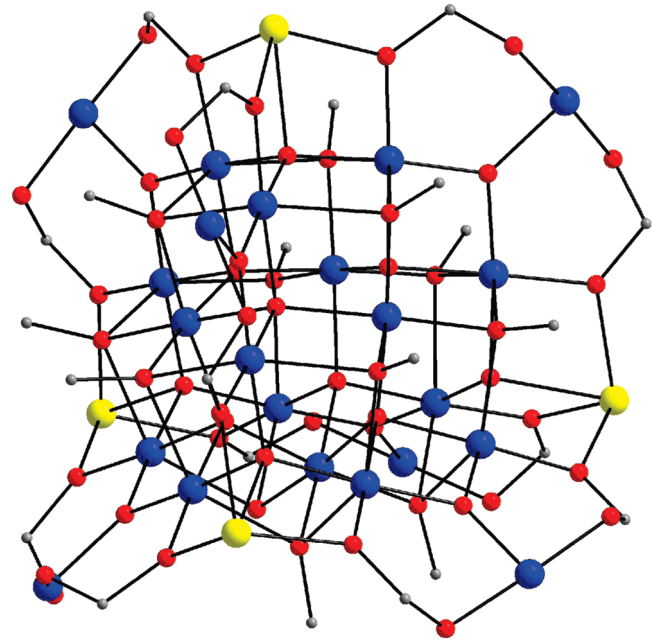

Figure 3. PovRay representation of the complete $[Mn_{26}(\mu_4\text{-}O)_{10}(\mu_3\text{-}O)_6(\mu_3\text{-}OMe)_{12}(\mu\text{-}OR)_{12}(OR)_{12}]^{6+}$ core of **3**; the $dpkd^{2-}$ ligands, except for their OR^- groups, have been omitted. Color scheme: Mn^{II}, yellow; Mn^{III}, blue; O, red; C, gray.

are thus $\eta^1{:}\eta^2{:}\eta^1{:}\eta^1{:}\mu_3$, where we are indicating the hapticity of each $dpkd^{2-}$ donor atom. The ligation is completed by a terminal MeOH (O7) group on each Mn2 atom, which hydrogen-bonds with one of the neighboring $dpkd^{2-}$ atoms, O2 (O7···O2 = 2.659 Å). Overall, the complex contains an $[Mn_{26}(\mu_4\text{-}O)_{10}(\mu_3\text{-}O)_6(\mu_3\text{-}OMe)_{12}(\mu\text{-}OR)_{12}]^{18+}$ core. If we consider the terminal alkoxide arm of each $dkpd^{2-}$ ligand as part of the core, then the description becomes $[Mn_{26}(\mu_4\text{-}O)_{10}(\mu_3\text{-}O)_6(\mu_3\text{-}OMe)_{12}(\mu\text{-}OR)_{12}(OR)_{12}]^{6+}$; the latter is shown in Figure 3. The core possesses T_d point group symmetry, but inclusion of the $dpkd^{2-}$ pyridyl groups removes the mirror planes and the complete cation thus possesses rare *T* symmetry, which is crystallographically imposed.

Charge considerations and an inspection of the metric parameters indicate a $4Mn^{II}$, $22Mn^{III}$ description for the cation of **3**. This was confirmed quantitatively by bond valence sum (BVS)[27] calculations (Table 3), which identified Mn1 as the Mn^{II} atom, and the others as Mn^{III} atoms. The latter was also consistent with the Jahn−Teller (JT) distortions at Mn2

(25) Brechin, E. K.; Sanudo, E. C.; Wernsdorfer, W.; Boskovic, C.; Yoo, J.; Hendrickson, D. N.; Yamaguchi, A.; Ishimoto, H.; Concolino, T. E.; Rheingold, A. L.; Christou, G. *Inorg. Chem.* **2005**, *44*, 502.
(26) Stamatatos, Th. C.; Poole, K. M.; Foguet-Albiol, D.; Abboud, K. A.; O'Brien, T. A.; Christou, G. *Inorg. Chem.* **2008**, *47*, 6593.
(27) (a) Brown, I. D.; Altermatt, D. *Acta Crystallogr.* **1985**, *B41*, 244. (b) Liu, W.; Thorp, H. H. *Inorg. Chem.* **1993**, *32*, 4102.
(28) (a) Chakov, N. E.; Lee, S.-C.; Harter, A. G.; Kuhns, P. L.; Reyes, A. P.; Hill, S. O.; Dalal, N. S.; Wernsdorfer, W.; Abboud, K. A.; Christou, G. *J. Am. Chem. Soc.* **2006**, *128*, 6975. (b) Stamatatos, Th. C.; Luisi, B. S.; Moulton, B.; Christou, G. *Inorg. Chem.* **2008**, *47*, 1134.
(29) For example, see: (a) Satcher, J. H., Jr.; Olmstead, M. M.; Droege, M. W.; Parkin, S. R.; Noll, B. C.; May, L.; Balch, A. L. *Inorg. Chem.* **1998**, *37*, 6751. (b) Stamatatos, Th. C.; Diamantopoulou, E.; Tasiopoulos, A.; Psycharis, V.; Vicente, R.; Raptopoulou, C. P.; Nastopoulos, V.; Escuer, A.; Perlepes, S. P. *Inorg. Chim. Acta* **2006**, *359*, 4194. (c) Hsieh, W.- Y.; Liu, S. *Inorg. Chem.* **2006**, *45*, 5034.

Table 3. Bond Valence Sum (BVS)[a,b] Calculations for Mn and O Atoms in **3**

atom	Mn^{II}	Mn^{III}	Mn^{IV}
Mn1	1.75	1.64	1.66
Mn2	3.06	2.83	2.91
Mn3	3.16	2.89	3.03
Mn4	3.13	2.87	3.01

	BVS	assignment	group
O1	1.78	RO^-	$dpkd^{2-}$
O2	1.68	RO^-	$dpkd^{2-}$
O3	1.95	O^{2-}	O^{2-}
O4	1.91	O^{2-}	O^{2-}
O5	1.88	O^{2-}	O^{2-}
O6	1.84	RO^-	MeO^-
O7	1.13	ROH	MeOH

[a] The underlined value is the one closest to the charge for which it was calculated. The oxidation state is the nearest whole number to the underlined value. [b] An O BVS in the ~1.8−2.0, ~1.0−1.2, and ~0.2−0.4 ranges is indicative of non-, single-, and double-protonation, respectively.

and Mn3, as expected for high-spin d^4 ions in near-octahedral geometry, taking the form of an axial elongation of the two *trans* $Mn-N_{py}$ (2.270(5) Å) and $Mn-O_{OMe}$ (2.296(4) and 2.306(4) Å) bonds. Thus, as is almost always the case, the JT elongation axes avoid the $Mn^{III}-O^{2-}$ bonds, the shortest and strongest in the molecule.[28] In contrast, Mn^{III} atom Mn4 possesses almost ideal MnO_6 octahedral geometry, as reflected in the six similar Mn−O distances (2.005, 2.006 Å) and the corresponding Mn−O−Mn angles (*cis* 85.4(2)−97.7(2)° and *trans* 175.0(2)°); this is, of course, the result of static disorder of the JT elongation about the three axes owing to Mn4 lying on the crystallographic C_3 symmetry axis. The Mn^{II} atoms are seven-coordinate with distorted pentagonal bipyramidal geometries. The protonation levels of O^{2-}, MeOH/MeO^-, and RO^- groups were confirmed by O BVS calculations (Table 3). Complex **3** does not form any significant intermolecular hydrogen bonds, only weak intermolecular contacts between C−H bonds and the π-system of $dpkd^{2-}$ groups.

Because the H atoms that are bound to O atoms were not crystallographically located, the alternative of formulating the complex as $[Mn_{26}O_{16}(OMe)_{18}(dpkd)_{12}]\cdot 6H_2O$, that is, as containing terminal methoxide ligands and lattice H_2O molecules, was also considered. However, we do not favor this possibility based on (i) the large Mn2−O7 distance (2.115(1) Å) which is indicative of a $Mn^{III}-O_{MeOH}$, rather than a $Mn^{III}-O_{MeO^-}$ bond;[30] (ii) the fact that methoxide ligands are normally bridging,[30,34] whereas O7 is terminally ligated to Mn(2), and (iii) the BVS value of O7 which suggests a neutral MeOH ligand rather than a methoxide. It should be mentioned that OH^- counterions are with precedent in cluster chemistry.[29] However, we anticipated that there would be other solvent molecules in the large voids present between cations (see Experimental Section) and these would be near to and hydrogen-bonding to the OH^- anions; unfortunately, this was not clear from the crystal structure, probably because of extensive disorder, but the elemental analysis data clearly indicate the presence of MeCN molecules on the basis of the N analysis.

Table 4. Chemical Formulas, Ground-State S Values, and U_{eff} Barriers for Polynuclear Mn Complexes with Nuclearities of 26 or More

complex[a,b]	S	U_{eff} (K)	ref
$[Mn_{26}O_{16}(OMe)_{12}(dpkd)_{12}(N_3)_6]$ (**1**)	~4	16.5[c]	20
$[Mn_{26}O_{16}(OH)_2(OMe)_{15}(dpkd)_{12}(H_2O)]^+$ (**2**)[a]	7	36.2[c]	20
$[Mn_{26}O_{16}(OMe)_{12}(dpkd)_{12}(MeOH)_6]^{6+}$ (**3**)[a]	6	30.0	t.w.
$[Mn_{26}O_8(OH)_4(N_3)_{12}(O_2CMe)_6(dpkd)_{14}(DMF)_4]$	8	46.0	21
$[Mn_{26}O_{17}(OH)_8(OMe)_4F_{10}(bta)_{22}(MeOH)_{14}(H_2O)_2]$	4	15.0	30
$[Mn_{30}O_{24}(OH)_8(O_2CCH_2Bu^t)_{32}(H_2O)_2(MeNO_2)_4]$	5	15.0	31
$[Mn_{32}(thme)_{16}(bpy)_{24}(N_3)_{12}(O_2CMe)_{12}]^{8+}$	~9	[d]	32
$\{[Mn_{10}O_2(O_2CMe)_{13}(pd)_6(py)_2]^-\}_4$	4	[d]	33
$[Mn_{84}O_{72}(O_2CMe)_{78}(OMe)_{24}(MeOH)_{12}(H_2O)_{42}(OH)_6]$	6	18	34

[a] Counterions and solvate molecules are omitted. [b] Abbreviations: t.w. = this work; btaH = benzotriazole; $thmeH_3$ = 1,1,1-tris(hydroxymethyl) ethane; bpy = 2,2′-bipyridine; pdH_2 = 1,3-propanediol; py = pyridine. [c] Calculated from bulk magnetic studies. [d] Non-SMM.

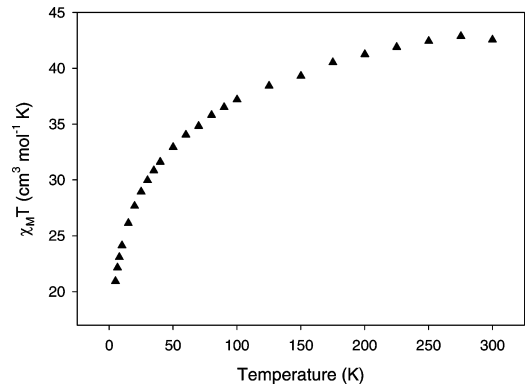

Figure 4. $\chi_M T$ vs T plot for **3**·3MeCN in a 1 kG dc field.

Complex **3** joins only a handful of previous manganese clusters with a nuclearity of 26 or larger. Most of these were reported only recently, and we have listed them in Table 4 for a convenient comparison of their formulas and pertinent magnetic data (S and U_{eff}; vide infra). Examination of Table 4 shows that the cation of **3** is one of the largest Mn clusters prepared to date, with only four known examples at higher nuclearity, including the $[Mn_{10}]_4$ complex that has a tetramer-of-clusters structure.

Magnetochemistry

Direct Current Magnetic Susceptibility Studies. Variable-temperature dc magnetic susceptibility (χ_M) measurements were performed on a powdered polycrystalline sample of dried complex **3**·3MeCN, restrained in eicosane to prevent torquing, in a 0.1 T field and in the 5.0−300 K range. The data are shown as a $\chi_M T$ versus T plot in Figure 4. $\chi_M T$ steadily decreases with decreasing temperature from 42.55 cm^3 K mol^{-1} at 300 K to 20.93 cm^3 K mol^{-1} at 5.0 K. The 300 K value is much less than the spin-only value of 83.5 cm^3 K mol^{-1} expected for a complex consisting of 4 Mn^{II} and 22 Mn^{III} noninteracting ions, indicating the presence of dominant antiferromagnetic exchange interactions within the cation. However, the 5.0 K value is still far from zero, suggesting that **3**·3MeCN possesses a fairly large ground-state spin value of $S = 6$ or 7; the spin-only ($g = 2$) values for $S = 6$ or 7 are 21 and 28 cm^3 K mol^{-1}, respectively.

(30) Jones, L. F.; Rajaraman, G.; Brockman, J.; Murugesu, M.; Sanudo, E. C.; Raftery, J.; Teat, S. J.; Wernsdorfer, W.; Christou, G.; Brechin, E. K.; Collison, D. *Chem.—Eur. J.* **2004**, *10*, 5180.
(31) Soler, M.; Wernsdorfer, W.; Folting, K.; Pink, M.; Christou, G. *J. Am. Chem. Soc.* **2004**, *126*, 2156.

Given the size of the Mn_{26} molecule, and the resulting number of inequivalent exchange constants, it is not possible to apply the Kambe method[35] to determine the individual pairwise Mn_2 exchange interaction parameters. We concentrated instead on characterizing the ground-state spin, *S*, and the zero-field splitting parameter, *D*, by performing magnetization (*M*) versus dc field measurements in the magnetic field and temperature ranges 1−70 kG and 1.8−10.0 K, respectively. However, we could not get an acceptable fit using data collected over the whole field range, which is a common problem caused by low-lying excited states, especially if some have an *S* value greater than that of the ground state, which is the case for **3**·3MeCN on the basis of Figure 4 and Supporting Information, Figure S1. A common solution is to only use data collected with low fields (≤1.0 T), as we previously reported for many mixed-valence Mn^{II}/Mn^{III} clusters.[8,9,25,31,36] However, it was still not possible to obtain a satisfactory fit assuming that only the ground state is populated in this temperature range. This suggests very low-lying excited states, which are populated even at these relatively low temperatures.

As we have described before on multiple occasions,[8,9,17a,25,31,32,36,37] ac susceptibility studies are a powerful complement to dc studies for determining the ground state of a system because they preclude any complications arising from the presence of a dc field. We thus carried out detailed ac studies on complex **3** as an independent determination of its ground-state *S*, and also to study magnetization dynamics.

Alternating Current Magnetic Susceptibility Studies. Alternating current studies were performed in the 1.8−15 K range using a 3.5 G ac field oscillating at frequencies (υ) in the 50−997 Hz range. If the magnetization vector can relax fast enough to keep up with the oscillating field, then there is no imaginary (out-of-phase) susceptibility signal (χ''_M), and the real (in-phase) susceptibility (χ'_M) is equal to the dc susceptibility. However, if the barrier to magnetization relaxation is significant compared to the thermal energy (kT), then χ'_M decreases and there is a non-zero χ''_M. In addition, χ''_M will be frequency-dependent. Such frequency-dependent χ''_M signals are a characteristic signature of the superparamagnetic-like properties of a SMM, but by themselves do not prove the SMM behavior.[33,38]

For complex **3**·3MeCN, the ac data are shown in Figure 5 and reveal several pertinent features: (i) $\chi'_M T$ (Figure 5, top) decreases almost linearly with decreasing temperature in the 7−15 K range, indicating depopulation of a high density of excited states with spin *S* greater than that of the ground state, in agreement with the conclusion from the dc studies. Below 7 K, $\chi'_M T$ decreases more rapidly because of ZFS and weak intermolecular interactions; (ii) extrapolation of the $\chi'_M T$ data from above ∼7.0 to 0 K, at which point only the ground state will be populated, gives a value of ∼21 $cm^3\ K\ mol^{-1}$, indicative of an $S = 6$ ground state with $g \sim 2.00$; (iii) below ∼4 K, there is a frequency-dependent decrease in $\chi'_M T$ and a concomitant appearance of frequency-dependent χ''_M signals (Figure 5, bottom); only the tails of peaks are visible above 1.8 K (the operating limit of our SQUID magnetometer), the peak maxima clearly lying at lower temperatures.

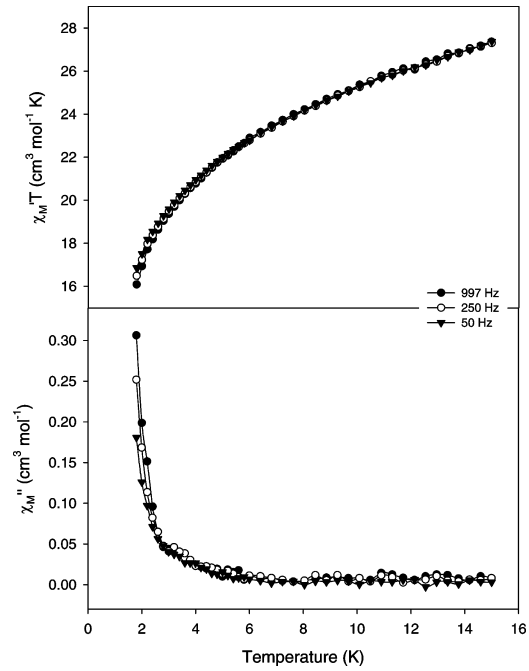

Figure 5. In-phase (χ'_M) (as $\chi'_M T$, top) and out-of-phase (χ''_M, bottom) vs *T* ac susceptibility signals for **3**·3MeCN in a 3.5 G field oscillating at the indicated frequencies.

Point (i) rationalizes the fact that we were unable to get a satisfactory fit of the dc magnetization data. The fitting procedure assumes only the ground state is populated, and its failure is clearly due to a combination of (a) many low-lying excited states, whose population is difficult to avoid even at the lowest temperatures employed, and (b) the larger *S* value compared with the ground state of at least many of these low-lying excited states will mean that M_S levels of the former will approach and even cross those of the latter, exacerbating the fitting difficulties. Of course, both (a) and (b) are to be anticipated for such a high nuclearity complex as **3**, especially given its content of Mn^{II} atoms, since these usually give very weak exchange interactions and small energy splitting. The ac experiment simplifies the situation by dispensing with the dc field completely: low-lying excited states then simply appear as a sloping $\chi'_M T$ versus *T* plot as their Boltzmann population changes, and extrapolation to 0 K, at which only the ground state will be populated, yields the true ground-state *S* value. The only problem that might occasionally appear is the presence of weak, usually anti-

(32) Scott, R. T. W.; Parsons, S.; Murugesu, M.; Wernsdorfer, W.; Christou, G.; Brechin, E. K. *Angew. Chem., Int. Ed.* **2005**, 6540.
(33) Moushi, E.; Lampropoulos, C.; Wernsdorfer, W.; Nastopoulos, V.; Christou, G.; Tasiopoulos, A. J. *Inorg. Chem.* **2007**, *46*, 3795.
(34) Tasiopoulos, A. J.; Vinslava, A.; Wernsdorfer, W.; Abboud, K. A.; Christou, G. *Angew. Chem., Int. Ed.* **2004**, *43*, 2117.
(35) Kambe, K. *J. Phys. Soc. Jpn.* **1950**, *5*, 48.
(36) (a) King, P.; Wernsdorfer, W.; Abboud, K. A.; Christou, G. *Inorg. Chem.* **2005**, *44*, 8659. (b) Tasiopoulos, A. J.; Wernsdorfer, W.; Abboud, K. A.; Christou, G. *Inorg. Chem.* **2005**, *44*, 6324.
(37) (a) Sanudo, E. C.; Wernsdorfer, W.; Abboud, K. A.; Christou, G. *Inorg. Chem.* **2004**, *43*, 4137. (b) Murugesu, M.; Raftery, J.; Wernsdorfer, W.; Christou, G.; Brechin, E. K. *Inorg. Chem.* **2004**, *43*, 4203.
(38) (a) Chakov, N. E.; Wernsdorfer, W.; Abboud, K. A.; Christou, G. *Inorg. Chem.* **2004**, *43*, 5919. (b) Mishra, A.; Tasiopoulos, A. J.; Wernsdorfer, W.; Abboud, K. A.; Christou, G. *Inorg. Chem.* **2007**, *46*, 3105.

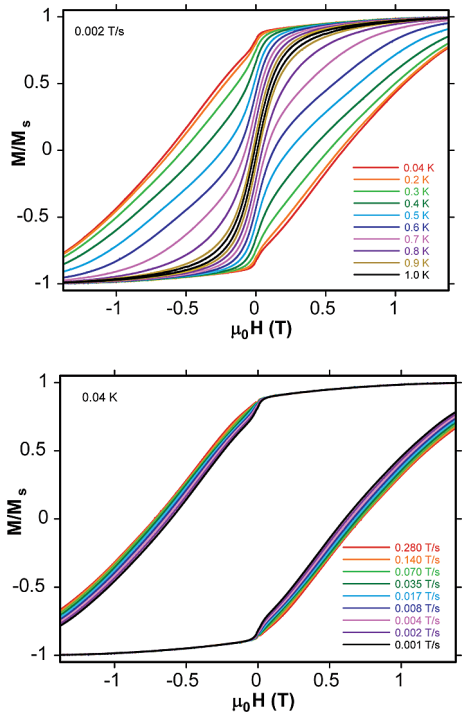

Figure 6. Magnetization (M) vs dc field hysteresis loops for a single crystal of **3**·solv at the indicated temperatures and a fixed field sweep rate of 0.002 T/s (top), and at the indicated field sweep rates and a fixed temperature of 0.04 K (bottom). The magnetization is normalized to its saturation value, M_S.

ferromagnetic, intermolecular exchange interactions, but even this can be circumvented by avoiding beginning the extrapolation at too low a temperature.

The χ''_M signals in Figure 5 (bottom) suggest but do not prove that complex **3** is an SMM. To confirm this, magnetization versus dc field sweeps were carried out at temperatures below 1.8 K to look for magnetization hysteresis, the diagnostic property of a magnet. Note that the previous Mn_{26} complexes **1** and **2** (Table 4) have the same core as the cation of **3**[20] but no hysteresis studies have been reported on them. The present studies on **3** were thus deemed important for all these Mn_{26} complexes, to provide a clear determination whether they really are SMMs or not, and if so, to study their quantum properties in detail and obtain a precise calculation of the effective energy barrier (U_{eff}) for the magnetization reversal.

Magnetization vs Applied dc Field Hysteresis Loops. Studies were performed on single crystals of **3**·solv at temperatures down to 0.04 K using a micro-SQUID apparatus.[24] The obtained magnetization versus applied dc field responses are shown in Figure 6, which includes both a temperature dependence at a constant field sweep rate of 0.002 T/s (Figure 6, top) and a field sweep rate dependence at a constant temperature of 0.04 K (Figure 6, bottom). Hysteresis loops were indeed observed below ~1.0 K, whose coercivities increase with decreasing temperature and increasing field sweep rate, as expected for the superparamagnetic-like properties of a SMM below its blocking temperature (T_B). The data thus confirm complex **3**·solv to be a new addition to the family of SMMs, with a blocking temperature (T_B) of ~1.0 K, above which there is no

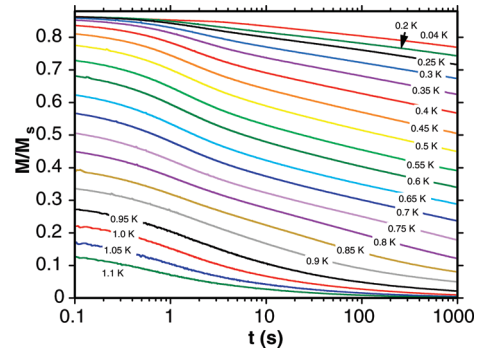

Figure 7. Magnetization (M) vs time decay plots in zero dc field for a single crystal of **3**·solv. The magnetization is normalized to its saturation value, M_S.

hysteresis. The loops do not show the steps characteristic of QTM, except for the one at zero field. This is as expected for high nuclearity SMMs since they are more susceptible to various step-broadening effects from low lying excited states, intermolecular interactions, and/or distributions of local environments owing to ligand and solvent disorder in the often large voids that contain disordered solvent of crystallization, as is the case for **3**·solv.[8,9,13d,21,34,39] The latter distribution of environments leads to a corresponding distribution in D values, and thus a broadening of the steps, sometimes to the point of being smeared beyond detection, because their exact position depends on D.

Relaxation Studies Using ac and dc Data. Two methods were combined to obtain a more quantitative assessment of the magnetization relaxation dynamics. Additional ac χ''_M studies were carried out on a single crystal of **3**·solv down to 1.0 K. At a given temperature, the position of the χ''_M peak maximum is the point at which the angular frequency ω ($\omega = 2\pi\upsilon$) of the oscillating field equals the magnetization relaxation rate ($1/\tau$, where τ is the relaxation time); relaxation rate versus T data can thus be obtained from the position of the peak maxima and this $\omega = 1/\tau$ relationship. For relaxation rate versus T data to lower temperatures, the crystal's magnetization was first saturated in one direction at ~5 K with a large applied dc field, the temperature decreased to a chosen value in the 0.04−1.1 K range, and then the field removed and the magnetization decay monitored with time. The resulting data are shown in Figure 7, from which were calculated the relaxation rate at the different temperatures.

The combined ac and dc relaxation rate ($1/\tau$) versus T data were used to construct an Arrhenius plot, shown as τ versus $1/T$ in Figure 8, using the Arrhenius relationship of eq 2a.

$$\tau = \tau_0 \exp(U_{eff}/kT) \quad (2a)$$

$$\ln(\tau) = \ln(\tau_0) + U_{eff}/kT \quad (2b)$$

The Arrhenius equation is appropriate for a thermally activated Orbach process, the characteristic behavior of an

(39) (a) Moushi, E. E.; Stamatatos, Th. C.; Wernsdorfer, W.; Nastopoulos, V.; Christou, G.; Tasiopoulos, A. J. *Angew. Chem., Int. Ed.* **2006**, *45*, 7722. (b) Murugesu, M.; Wernsdorfer, W.; Abboud, K. A.; Brechin, E. K.; Christou, G. *Dalton Trans.* **2006**, 2285. (c) Wittick, L. M.; Murray, K. S.; Moubaraki, B.; Batten, S. R.; Spiccia, L.; Berry, K. J. *Dalton Trans.* **2004**, 1003.

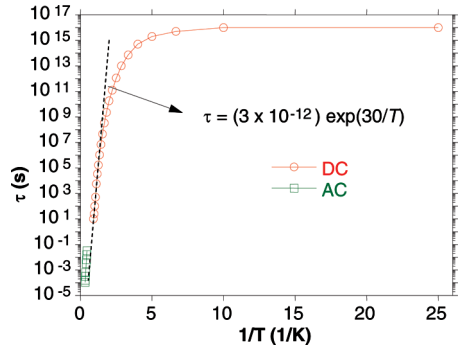

Figure 8. Arrhenius plot of the relaxation time (τ) vs $1/T$ for a single crystal of **3**·solv using data obtained from ac susceptibility and the dc magnetization decay measurements of Figure 7. The dashed line is the fit of data in the thermally activated region to the Arrhenius equation; see the text for the fit parameters.

SMM, where U_{eff} is the effective energy barrier and k is the Boltzmann constant. The fit to the thermally activated region above ~0.1 K gave $\tau_0 = 3.0 \times 10^{-12}$ s and $U_{eff} = 30$ K. A U_{eff} of 30 K is one of the highest ever reported for a Mn(II,III) mixed-valent complex, although still significantly smaller than the Mn^{III}_6 (86 K)[40] and $Mn^{III/IV}_{12}$ (74 K)[28a] complexes. The τ_0 is smaller than normally seen for SMMs, but this is sometimes the case for the larger, higher nuclearity ones.[9,41] At ~0.1 K and below, the relaxation becomes temperature-independent, consistent with relaxation by ground-state QTM. In other words, tunneling is now only between the lowest-energy $M_s = \pm 6$ levels of the $S = 6$ manifold, and no longer via a thermally (phonon) assisted pathway involving higher-energy M_s levels.

Conclusions

The present extension of the use of dpk-derived ligands in Mn cluster chemistry is a further demonstration of the ability of this group to foster formation of very high nuclearity products. To date, the use of dpk in reactions with a variety of Mn sources has provided six clusters, $[Mn^{II}_{10}Mn^{III}_4O_4(O_2CMe)_{20}(dpkdH)_4]$,[19] $[Mn^{II}_4Mn^{III}_{22}O_{16}(OMe)_{12}(dpkd)_{12}(N_3)_6]$ (**1**),[20] $[Mn^{II}_4Mn^{III}_{22}O_{16}(OH)_2(OMe)_{15}(dpkd)_{12}(H_2O)](ClO_4)$ (**2**),[20] $[Mn^{II}_4Mn^{III}_{22}O_{16}(OMe)_{12}(dpkd)_{12}(MeOH)_6](OH)_6$ (**3**), $[Mn^{II}_4Mn^{III}_{20}O_{10}(N_3)_8(O_2CBu^t)_{16}(dpkd)_{12}(DMF)_4]$,[21] and $[Mn^{II}_{12}Mn^{III}_{14}O_8(OH)_4(N_3)_{12}(O_2CMe)_6(dpkd)_{14}(DMF)_4]$.[21] It is also clear from Table 4 that four of the nine Mn_x complexes with $x \geq 26$ contain $dpkd^{2-}$ as one of the main bridging/chelating ligands. Complex **3** has the same core as **1** and **2**[20] but different peripheral ligation, and it thus increases to three the members of this still small family of $Mn^{II}_4Mn^{III}_{22}$ non-carboxylate clusters. The magnetization hysteresis loops for **3** unequivocally confirm that it is an SMM, and by implication confirms that **1** and **2** are also SMMs. Note that complex **3** possesses a large U_{eff} value for a $Mn^{II/III}$ cluster; the many low-lying excited states typical of $Mn^{II/III}_x$ SMMs normally preclude significant effective barriers compared with Mn^{III}_x and $Mn^{III/IV}_x$ SMMs. However, this work and recent reports[20,21] show that some high-nuclearity $Mn^{II/III}$ clusters can indeed exhibit significant U_{eff} barriers. Finally, it will be interesting to see in the future to what extent $dkpd^{2-}$ will continue to provide new high nuclearity Mn_x clusters, as large as or even larger than those identified to date.

Acknowledgment. This work was supported by EPEAEK II (Program PYTHAGORAS I, Grant b.365.037 to S.P.P.), the Cyprus Research Promotion Foundation (Grant TEXNO/0506/06 to A.J.T.), and NSF (Grant CHE-0414555 to G.C.).

Supporting Information Available: X-ray crystallographic file in CIF format for complex **3**·solv and magnetization versus magnetic field plot of dried **3**·3MeCN at 1.8 K. This material is available free of charge via the Internet at http://pubs.acs.org.

IC801342F

(40) Milios, C. J.; Vinslava, A.; Wernsdorfer, W.; Moggach, S.; Parsons, S.; Perlepes, S. P.; Christou, G.; Brechin, E. K. *J. Am. Chem. Soc.* **2007**, *129*, 2754.
(41) Stamatatos, T. C.; Abboud, K. A.; Wernsdorfer, W.; Christou, G. *Polyhedron* **2007**, *26*, 2095.